International Journal of Precision Engineering and Manufacturing
https://doi.org/10.1007/s12541-020-00356-2

Online ISSN 2005-4602
Print ISSN 2234-7593

REGULAR PAPER

An Efficient Parallel Infilling Strategy and Its Application in Sheet Metal Forming

Yan-Min Xie[1] · Yuan-Heng Guo[1] · Fei Zhang[1] · Yue-Peng Yue[1] · Mei-Qiang Feng[1] · Jiang-Bo Zhao[1]

Received: 14 March 2019 / Revised: 3 April 2020 / Accepted: 26 April 2020

Abstract

Infilling strategies play an important role in kriging based optimization, especially when computationally expensive simulations are involved. In order to improve the efficiency of constructing a high-precision kriging model, an improved expected improvement criterion (IEI) and a parallel infilling strategy are proposed based on the maximum expected improvement (EI) criterion. In the proposed parallel infilling strategy, new sample points are generated by employing IEI criterion coupled with EI criterion. During the improved sampling process, redundant and pseudo sample are deleted in order to avoid failure of constructing a kriging model. An improved weighted particle swarm optimization (WPSO) algorithm is proposed to improve optimization efficiency. The proposed parallel infilling strategy is applied to nonlinear function optimization and variable blank holder force (VBHF) optimization in a double-c stamped part. Based on the LHD and software DYNAFORM, kriging models between the VBHF and forming quality are constructed. Compared with the initial kriging models, the meat relative error of kriging models with the proposed parallel infilling strategy for the wrinkling and average thinning rate are reduced by 95% and 55%, respectively. The optimal VBHF is obtained by the WPSO. The results show that, cracking has been completely eliminated and wrinkling has been decreased, greatly improving the forming quality of the double-c stamped part.

Keywords Kriging model · Parallel infilling strategy · Variable blank holder force · Sheet metal forming

List of Symbols

$\mathbf{f}^{\mathrm{T}}(x)$	Regression models in kriging
$\boldsymbol{\beta}$	An undetermined regression coefficient
$\mathbf{R}(\mathbf{x}, \mathbf{w})$	The spatial correlation function that only depends on the Euclidean distance between two sites $\boldsymbol{x}$ and $\boldsymbol{w}$
N	The number of sample points constructing a kriging model
$\boldsymbol{\sigma}_z^2$	Variance
$\hat{\boldsymbol{\sigma}}_z^2$	The estimated value of variance
$\boldsymbol{X}$	The experimental points
$\boldsymbol{Y}$	The experimental responses
$\boldsymbol{R}$	The correlation matrix between $\boldsymbol{X}$
$\boldsymbol{r}$	The correlation matrix between the test points and experimental points
$y(x)$	The real response
$\hat{y}(x)$	The predictive value of a kriging model
$s^2(x)$	The predictive variance of a kriging model
$\boldsymbol{\Phi}(\cdot)$	The standard normal cumulative distribution function
$\phi(\cdot)$	The standard normal probability density function
y_{kri}	The best observed value
y'_{kri}	The maximum kriging prediction value
ε	A decimal to keep the denominator from zero when the real response is 0
n	The number of test points
$\boldsymbol{d}$	The distance between the tested sample points and the original sample points
$\boldsymbol{\theta}$	The key parameter of a kriging model
MRE	The mean relative error
y	The thinning rate value
q	The wrinkling value

1 Introduction

Surrogate model technology is an effective way to reduce computational cost in engineering optimization. As an increasingly mature surrogate model, kriging models have

✉ Yan-Min Xie
xie_yanmin@swjtu.edu.cn

[1] School of Mechanical Engineering, Southwest Jiaotong University, No. 111, North 1st Section of Second Ring Road, Jinniu District, Chengdu 610031, China

Published online: 18 May 2020

been developed in depth. Liu et al. [1] proposed a gradient-enhanced kriging method and Han et al. [2] applied the method into aerodynamic inverse design, proving that the gradient-enhanced kriging model could solve higher dimensional problems than the ordinary kriging method. Kennedy and O'Hagan [3] developed a co-kriging method and Elsayed [4] optimized the cyclone separator geometry with the co-kriging method. Roshan et al. [5] presented a blind kriging method, which showed remarkable improvement in prediction accuracy. Due to the complexity of engineering problems, the ordinary kriging model has more extensive applications. Hamza et al. [6] applied an ordinary kriging model coupled with level set methods into structural topology optimization. Based on kriging models and genetic algorithms, Yang et al. [7] optimized the gear modification and the total computation time was reduced from 26.91 days to 2.24 h compared to the finite element method. Xie [8] established a robust kriging model and applied the model in sheet metal forming process. Kim et al. [9] proposed an efficient multi-objective optimization approach for a plasmonic nanoslit array sensor using kriging surrogate models. Li et al. [10] studied multi-objective optimization of heating, ventilation and air conditioning (HVAC) system using the non-dominated sorting-based particle swarm optimization (NSPSO) and kriging models. Abebe et al. [11] optimized multi-point forming process based on kriging models.

In general, high-precision kriging models are required for complex engineering problems. After initial kriging models are constructed, new samples need to be added repeatedly based on sampling strategies to update the models.

Traditional sampling strategies are single point sampling strategies. Only one new sample is added in a single sampling strategy. The most widely used criterion is the maximum expected improvement (EI) criterion, which was presented by Jones et al. [12]. It has good global search performance but its local convergence is not satisfactory. Jones also proposed the minimum prediction (MP) criterion, which can easily get stuck in the local minimum. Forrester et al. [13] put forward a maximum probability improvement (PI) criterion and a maximum mean square error (MSE) criterion. PI has the same performance as the EI criterion. Laurenceau et al. [14] developed a minimum lower confidence boundary (LCB) criterion. Liu et al. [15] proposed a novel adaptive sampling strategy by maximizing the expected prediction error and they proved its high efficiency. Jia et al. [16] developed a new sampling criterion which was called the reliability infill sampling criterion. These methods mentioned above have a common feature, that is, only one new point is chosen in each updating cycle, and kriging models have slow convergence.

To improve the efficiency of the single point infilling strategy, there are some multi-point infilling criteria. Chaudhuri et al. [17] got multiple new points through combining the EI with the PI to optimize flapping wings. Liu et al. [18] combined the four existing criteria (EI, PI, MP, and LCB) and applied this strategy into aerodynamic shape optimization of transonic wings. The result showed that it was more efficient than single sampling criteria. Based on the MP criterion, Gao and Wang [19] presented a new multi-point infilling criterion and it was used to optimize injection molding process. Ginsbourger et al. [20] developed a q-EI strategy using a generalized EI strategy defined by Schonlau [21]. In this proposed strategy, a highly expensive computational method such as Monte-Carlo simulation was needed to derive the solutions of multiple EI criteria. Clément and Ginsbourger [22] proposed a new way of computing q-EI without using Monte-Carlo simulations through a closed-form formula, and demonstrated that the method had a very fast computation of q-EI. Viana and Haftaka [23] used the PI criterion to select multiple points from Monte Carlo sampling, and they found that more sample points were filled in each updating cycle, and the less iteration was usually needed. Yao et al. [24] showed a hybrid infilling strategy by combining the LCB with the Divergence from local Linear Interpolation (DLI) criteria. Based on the EI function, a multi-point infilling strategy was proposed by Cai et al. [25], which could intelligently generate new samples in an area with the certain probability according to corresponding EI values. They found it was very suitable for design optimization problems involving computationally expensive simulations. Desautels et al. [26] proposed a parallel selection method to parallelize exploration–exploitation tradeoffs in Gaussian process bandit optimization. Based on multi-objective optimization front, Ma et al. [27] developed a multi-points sampling criterion and the result showed that the number of infilling iterations for the proposed infilling strategy was only 17% that of the EI strategy. Wu et al. [28] developed a parallel knowledge gradient method, and the method could found global optimal values significantly faster than previous batch Bayesian optimization algorithms.

In this paper, to improve the accuracy and efficiency of constructing kriging models, an improved EI (IEI) criterion is proposed, and a parallel infilling strategy is developed at the same time. Classical nonlinear functions are used to verify the effectiveness of the parallel infilling strategy, and then this method is applied to the optimization of variable blank holder forces. The remainder of the paper is organized as follows. The IEI criterion and the novel parallel infilling strategy are introduced in Sect. 2. In Sect. 3, the proposed parallel infilling strategy is applied to classical nonlinear function optimization and the effectiveness of the IEI criterion and the proposed parallel infilling strategy are validated. In Sect. 4, the proposed parallel infilling strategy is applied to optimization of variable blank holder forces in a double-c stamped part. Concluding remarks are provided in Sect. 5.

2 A New Parallel Filling Strategy

2.1 Kriging Models

Kriging models were first presented by Krige [29]. Though it has been developed in depth, only the ordinary kriging is chosen in this paper, and its basic form is as follow:

$$y = \mathbf{f}^{\mathrm{T}}(x)\boldsymbol{\beta} + z(x) \tag{1}$$

where the order of $\mathbf{f}^{\mathrm{T}}(x)$ can be 0, 1 or 2 and in this paper is 0; $z(x)$ is a stochastic process with mean zero and variance $\boldsymbol{\sigma}_z^2$. The covariance is defined as:

$$\mathrm{cov}(z(\mathbf{x}), z(\mathbf{w})) = \boldsymbol{\sigma}_z^2 \mathbf{R}(\mathbf{x}, \mathbf{w}) \tag{2}$$

here the Gauss function is chosen as the correlation function.

Based on the generalized least squares estimation method, the estimated $\boldsymbol{\beta}$ value is:

$$\hat{\boldsymbol{\beta}} = \left(\mathbf{X}^{\mathrm{T}}\mathbf{R}^{-1}\mathbf{X}\right)^{-1}\mathbf{X}^{\mathrm{T}}\mathbf{R}^{-1}\mathbf{Y} \tag{3}$$

The estimated value of $\boldsymbol{\sigma}_z^2$ is:

$$\hat{\boldsymbol{\sigma}}_z^2 = \frac{1}{N}(\mathbf{Y} - \mathbf{X}\boldsymbol{\beta})^{\mathrm{T}}\mathbf{R}^{-1}(\mathbf{Y} - \mathbf{X}\boldsymbol{\beta}) \tag{4}$$

Based on the obtained model coefficient and correlation function parameters, the predictive value of a kriging model at the unknown point x_0 is:

$$\hat{y}(x_0) = \mathbf{f}^{\mathrm{T}}(x_0)\boldsymbol{\beta} + \mathbf{r}^{\mathrm{T}}(x_0)\mathbf{R}^{-1}(\mathbf{Y} - \mathbf{X}\boldsymbol{\beta}) \tag{5}$$

2.2 Maximum Expected Improvement Criterion (EI)

Sampling criteria are the base of obtaining new sample points when updating the kriging model. This can improve the efficiency of constructing a kriging model. Suppose a random variable $Y \sim [\hat{y}(x), s^2(x)]$, the improvement can be defined as $I = y_{kri} - \hat{y}(x) > 0$, so the maximum expected improvement (EI) can be given by [12]:

$$Max: \quad E[I(x)] = \begin{cases} (y_{kri} - \hat{y}(x))\boldsymbol{\Phi}\left(\frac{y_{kri} - \hat{y}(x)}{s(x)}\right) \\ \quad + s(x)\phi\left(\frac{y_{kri} - \hat{y}(x)}{s(x)}\right) & if \;\; s(x) > 0 \\ 0 & if \;\; s(x) = 0 \end{cases} \tag{6}$$

2.3 An Improved EI Criterion (IEI)

The maximum expected improvement sampling strategy is used to search for the points with a smaller value or greater variance than the current local optimal point. Henkenjohann et al. [30] proposed a criterion defined as:

$$I(x) = \begin{cases} y_{\max} - \hat{y}(x) & if \;\; y_{\max} > \hat{y}(x) \\ 0 & if \;\; y_{\max} < \hat{y}(x) \end{cases} \tag{7}$$

Where $y_{\max}$ is the maximum of current real objective values. In this paper, a new adaptive sampling infilling strategy is proposed, which has a strong ability to search for maximum areas. In the proposed criteria, the constrains in Eq. (7) are replaced with $s(x)$. The expression of the improved adaptive sampling criterion (IEI) is given by:

$$Max: \quad E[I(x)] = \begin{cases} (\hat{y}(x) - y'_{kri}) \times \left(1 - \boldsymbol{\Phi}\left(\frac{\hat{y}(x) - y'_{kri}}{s(x)}\right)\right) \\ \quad + s(x) \times \phi\left(\frac{\hat{y}(x) - y'_{kri}}{s(x)}\right) & if \;\; s(x) > 0 \\ 0 & if \;\; s(x) = 0 \end{cases} \tag{8}$$

2.4 The Proposed Parallel Infilling Strategy

In the paper, a new parallel infilling strategy is proposed. Multiple new samples are added to update a kriging model in each updating cycle by the strategy. The flowchart is shown in Fig. 1.

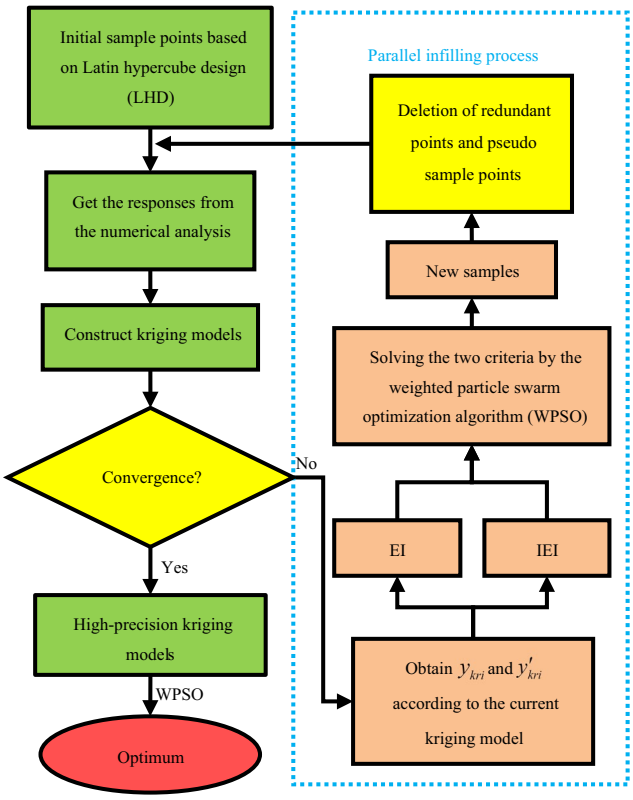

Fig. 1 The flowchart of the proposed parallel sampling strategy

2.4.1 The Convergence Criterion

The convergence criterion in this paper refers to stopping adding new points when the mean relative error (MRE) of a kriging model is less than 0.05, and it means that the error limit is 5%. The MRE can be calculated as:

$$MRE = \frac{1}{n}\sum_{i=1}^{n}\frac{|y(x)-\hat{y}(x)|}{|y(x)+\varepsilon|}, \quad \varepsilon = \begin{cases} 0 & |y(x)\neq 0| \\ 0.01 & |y(x)=0| \end{cases} \tag{9}$$

2.4.2 Deletion of Redundant Points and Pseudo Sample Points (PSP)

Based on the proposed parallel filling strategy, multiple new points are generated to update the kriging model in each updating cycle. It is possible that there are redundant sample points which should be deleted. The deletion of redundant points consists of two cases. The first case is to delete duplicate points between the new sampling points and another case is the deletion of the duplicate points between the new sample points and the initial sample points. In this paper, the Gauss function (the correlation function in a kriging model) is used to complete the deletion of redundant points. The Gauss function can be given by [29]:

$$\begin{aligned} R &= \exp\left(-\theta_j d_j^2\right) \\ d_j &= w_j - x_j \end{aligned} \tag{10}$$

where R means the degree of correlation between two points, and $R \in [0, 1]$. w are the original samples, x are the tested samples. When the distance between the two sample points is large, R is close to 0; when the distance between the two sample points is close to 0, R is close to 1; when the two points are completely overlapped, the correlation is maximum $R=1$.

The pseudo sample points (PSP) are proposed in the optimization of an engineering case studied in this paper. Different from the redundant points which make the kriging modeling process directly fail, PSPs can make the model response severely invalid. This phenomenon is more evident in the engineering case studied in this paper, therefore the PSPs will be introduced in detail during the engineering case optimization.

2.4.3 The Weighted PSO

In order to improve the accuracy of the optimal solution which is obtained by an optimization algorithm, the weighted particle swarm optimization (WPSO) algorithm is proposed in this paper. In the general PSO, the speed and location of the particle can be updated by [31]:

$$\begin{aligned} v_{ij}(t+1) &= v_{ij}(t) + c_1 r_1(p_{ij} - x_{ij}(t)) + c_2 r_2(p_g - x_{ij}(t)) \\ x_{ij}(t+1) &= x_{ij}(t) + v_{ij}(t+1) \end{aligned} \tag{11}$$

where v is the particle speed, x is the particle location coordinates. c_1 and c_2 are the learning factors which are constant and belong to [0, 2]. r_1 and r_2 are pseudo-random numbers and meet uniform distribution on [0, 1]. p_g is the global optimum.

In the WPSO, the learning factors c_1 and c_2 vary during the iteration, and they can be updated in the ith iteration by:

$$c_k = c_{\max} + \frac{(c_{\min} - c_{\max})(i_{\max} - i)}{i_{\max}}, \quad k = 1,\ 2 \tag{12}$$

where $c_{\max}$ is the upper limit of the learning factors and $c_{\min}$ is the lower limit. $i_{\max}$ is the maximum iteration in the algorithm, and i is the ith iteration.

The updated speed in the WPSO can be defined as:

$$\begin{aligned} v_{ij}(t+1) &= w v_{ij}(t) + c_1 r_1(p_{ij} - x_{ij}(t)) + c_2 r_2(p_g - x_{ij}(t)) \\ w &= w_{min} + (w_{\max} - w_{min})\text{rand} + 0.1\text{randn} \end{aligned} \tag{13}$$

where w is the variable weight coefficient in the optimization process. $w_{\max}$ is the upper limit and $w_{\min}$ is the lower limit. *rand* is a function which can produce a pseudo-random number belong to [0, 1], and *randn* is a function that generate a pseudo-random number belong to [− 1, 1]. Besides, the initial population in the general PSO is generated by random such as through a *rand* function in Eq. (13), while the initial population in the WPSO is generated by the Latin hypercube design (LHD) [32], which can help improve the uniformity of the initial population.

To compare WPSO with the general PSO, the Ackley function is optimized by the two algorithms. The function can be given as:

$$\begin{aligned} f(x) = -dexp\left(-0.2\sqrt{\frac{1}{m}\sum_{j=1}^{m}x_j^2}\right) - \exp\left(\frac{1}{m}\sum_{j=1}^{m}\cos(2\pi x_j)\right) \\ + e + f, \quad x_j \in [-1, 1] \end{aligned} \tag{14}$$

where e is 20, f is 2.71282, and m is 2 in this case. The optimum is 0. The best solutions obtained by the two algorithms

Table 1 The optimal solutions obtained by the two algorithms

	The optimal solutions
PSO	(0.0057, 0.0003)
WPSO	(− 0.0026, − 6.049e−05)

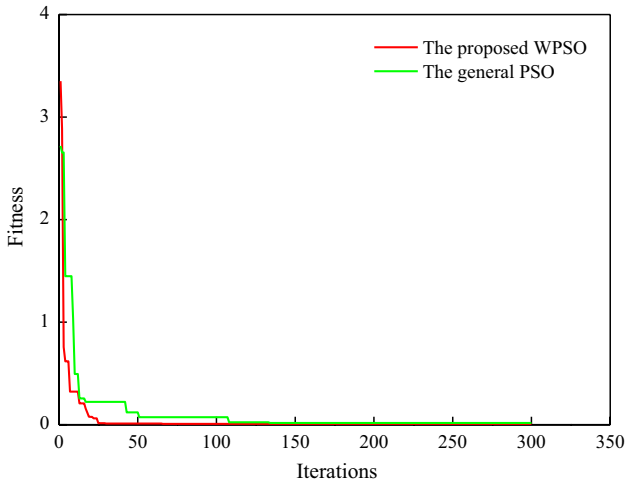

Fig. 2 The fitness curves of the two algorithms

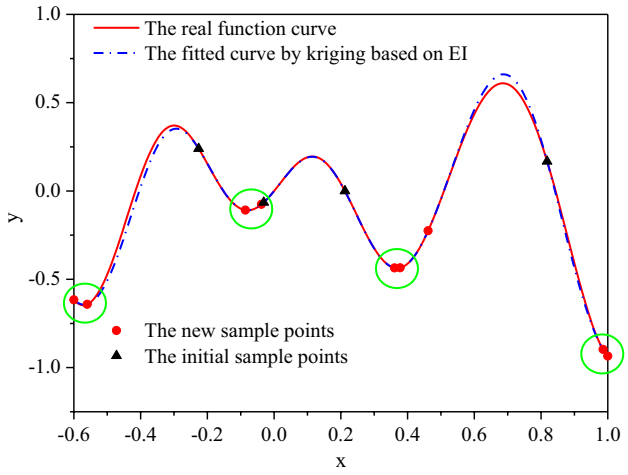

Fig. 3 The curve fitted by the kriging model based on the EI criterion. (Color figure online)

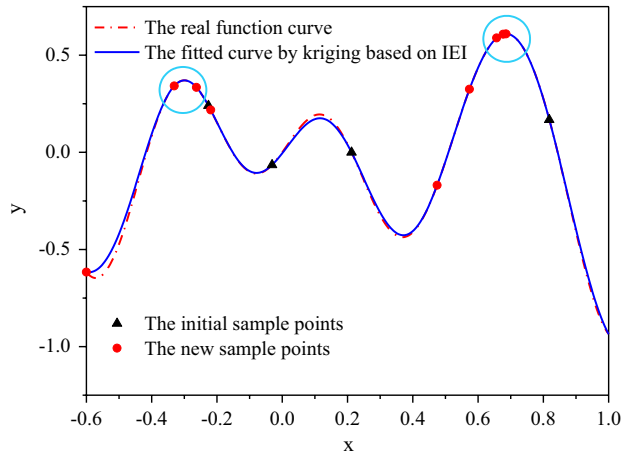

Fig. 4 The curve fitted by the kriging model based on the IEI criterion. (Color figure online)

are showed in Table 1. The fitness curves of the two algorithms are showed in Fig. 2.

According to the above results, it can be seen that the accuracy and the convergence speed of the WPSO are higher than the general PSO.

3 Verification of the Parallel Infilling Strategy

3.1 Verification of the IEI Criterion

Firstly, an initial kriging model has been constructed for a univariate function, then the EI criterion and IEI criterion are used successively. The univariate function is as follow:

$$f(x) = x\sin(10x + 1) + 0.1\sin(15x), \quad x \in [-0.6, 1] \tag{15}$$

For the comparison, 4 initial sample points are taken based on the LHD and only 9 iterations are allowed for the two criteria. Another 10 points are taken as the validation samples, and the MRE of the kriging model is calculated by Eq. (9). The curve fitted by the kriging model based on the EI criterion is shown in Fig. 3. The fitted curve based on the IEI criterion is shown in Fig. 4. Table 2 is the comparison of the kriging model accuracy based on the two kinds of sampling criteria.

From Table 2, the accuracy of the kriging model using the improved filling criterion is higher than that of the EI. Figures 3 and 4 show that the EI criterion performs better for searching local minimum (the green circles in Fig. 3), but the IEI criterion performs better for global maximum (the blue circles in Fig. 4). So in the proposed parallel infilling strategy, the purpose of EI criteria is to find a minimum, however the purpose of the IEI criteria is to find a maximum.

Table 2 Comparison of the kriging model accuracy based on the two kinds of sampling criteria

	Iterations	MRE (%)
EI	9	11
IEI	9	5.01

3.2 Verification of the Proposed Parallel Infilling Strategy

In this section, Colville function is successively optimized by using the single infilling strategy (the EI strategy) and the proposed parallel infilling strategy (EI and IEI).

The Colville function can be defined as follows:

Table 3 Comparison of the optimization results for the Colville function

	Single infilling strategy	Parallel infilling strategy
Iterations	47	34
MRE	2.55%	0.99%
Optimal value	0.0087	0.0056

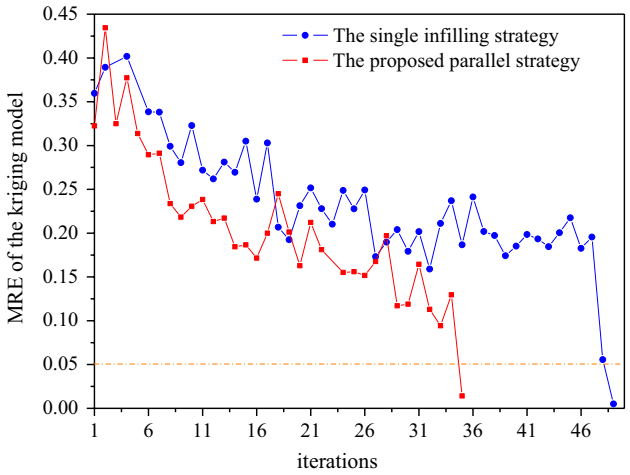

Fig. 5 Comparison of the convergence process based on the two kinds of sampling strategies for the Colville function

Table 4 Comparison of modeling results based on the two kinds of sampling strategies

	Single infilling strategy	Parallel infilling strategy
Number of sample points	107	101
CPU time (s)	230	200

$$y = 100(x_1^2 - x_2)^2 + (x_1 - 1)^2 + 90(x_3^2 - x_4) + 10.1\left((x_2 - 1)^2 + (x_4 - 1)^2\right) + 19.8(x_2 - 1)(x_4 - 1)$$
$$x_{1,2,3,4} \in [-10, 10], y_{optimum} = 0 \quad (16)$$

60 sample points are taken as the initial samples based on the LHD. The modeling results are presented in Table 3 and the convergence process of the two models are shown in Fig. 5.

When the convergence criterion is met, the total number of the sample points and the total CPU time spent on the same computer based on the two sampling strategies can be shown in Table 4.

From the Table 3, compared with the single filling strategy, the number of iterations with the parallel strategy is reduced by approximately 27%, and the accuracy is increased by approximately 61%. From Fig. 5, it shows that the convergence of the proposed parallel strategy is faster than that of the single infilling strategy. Table 4 shows that the total number of samples required for modeling in the parallel strategy is less than that of the single infilling strategy and the total CPU time in the parallel infilling strategy is shorter (reduced by 13%). From all the above results, the optimum value can be obtained quickly by the parallel strategy, and the accuracy of the corresponding kriging model is higher.

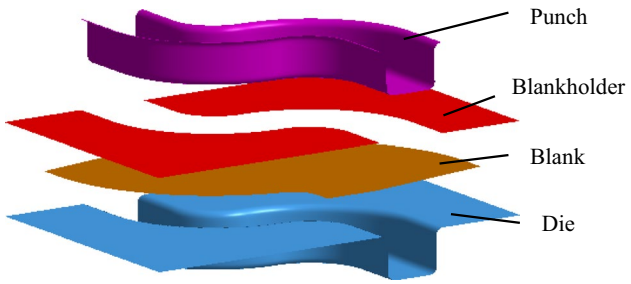

Fig. 6 The finite element model of the double-c

Table 5 The material parameters and process parameters

Parameters	Values
Initial blank holder force: F/kN	350
Coulomb friction coefficient: μ	0.125
Thickness: t/mm	1.00
Density: ρ/g cm^{-3}	7.85
Young's modulus: E/GPa	207
Poisson's ratio: v	0.28
R_{00}	2.48
R_{45}	2.27
R_{90}	2.65

4 Multi-objective Optimization of VBHF

A double-c stamped part is taken as the engineering case in this paper. Deep drawing of the double-c part is simulated by the software DYNAFORM.

4.1 Validation of the Finite Element Model

The finite element model in DYNAFORM is shown in Fig. 6. The material is DC03 cold rolled steel, and the stress–strain curve of the material is $\sigma = 540.7(0.005815 + \varepsilon_p)^{0.21}$MPa, and other material parameters of the blank and process parameters are given in Table 5 [33].

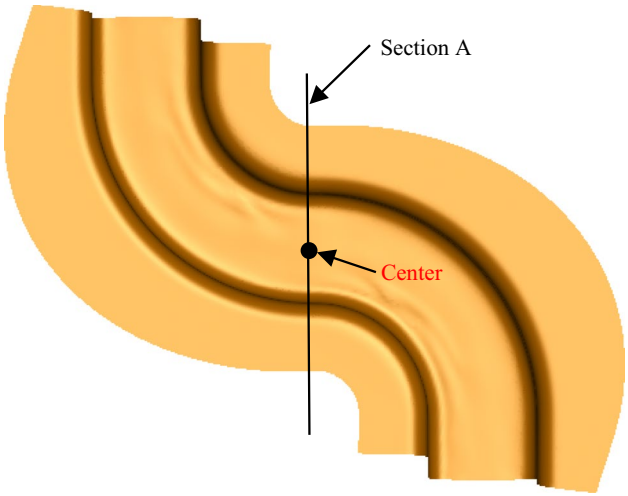

Fig. 7 The location of the section A

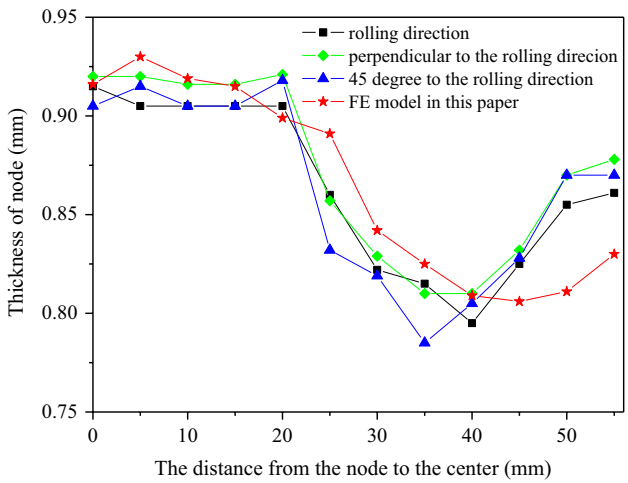

Fig. 8 The thickness distribution in the section A

The punch stroke is 40 mm, and the constant blank holder force is 350 KN. To verify the effectiveness of the finite element model, the thickness distribution of the section A has been obtained from the simulation and experiment. In the experimental samples, the material anisotropy is taken into consideration including the rolling direction, vertical direction and 45° to the rolling direction. The location of the section A is shown in Fig. 7. For the symmetry of the section, its half is chosen for thickness measurement, and the comparison between the simulation and the experiment can be seen in Fig. 8. It can be known from Fig. 8 that the thickness distribution of the section by the finite element numerical simulation is basically consistent with the experimental results, proving the effectiveness of the finite element model.

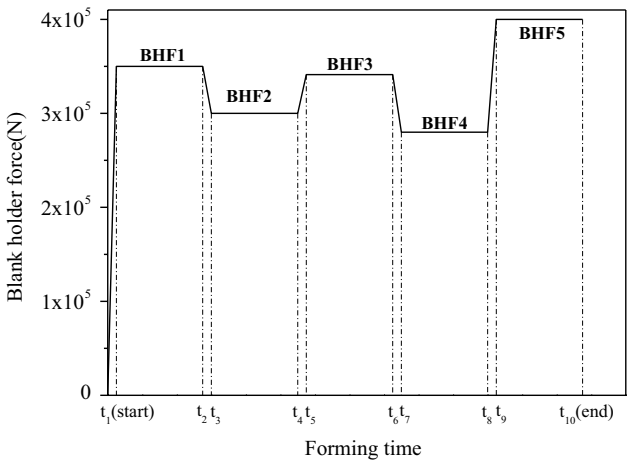

Fig. 9 The variable blank holder forces

Table 6 The range of the five BHFs (unit: KN)

	BHF1	BHF2	BHF3	BHF4	BHF5
Min	200	200	200	200	200
Max	450	450	450	450	450

4.2 Multi-objective Optimization of VBHF Based on the Parallel Infilling Strategy

4.2.1 Variable Blank Holder Force

Blank holder forces (BHFs) are set to prevent the blank from cracking and wrinkling in the forming process. With the development of modern technology, the traditional constant BHF loading method cannot meet forming quality requirements of stamped parts, so the VBHF method is proposed.

The VBHF means that the BHF can be changed with the punch stroke. The proposed parallel infilling strategy and kriging models are employed to optimize the VBHF in the sheet metal forming. Figure 9 shows that how the BHF varies in the forming stage.

In the forming process, there are five BHFs which are shown in Fig. 9, and the ranges of their values are shown in Table 6.

4.2.2 The Optimization Objectives

In this paper, the average thinning rate and the wrinkle value are taken as the optimization objectives. Two kriging models need to be established. One is between the VBHF and the average thinning rate, and the other is between the VBHF and the wrinkling value.

The average thinning rate can be defined as:

$$y_t = \frac{1}{n}\sum_{i=1}^{n}\left(\frac{t_i - t_0}{t_0}\right)^2 \tag{17}$$

where t_0 is the initial blank thickness, t_i is the thickness of ith element, and n is the total number of the stamped double-c elements.

For the wrinkling limit curve approximates a straight line, it can be expressed as:

$$\varepsilon_1 = -\varepsilon_2(\varepsilon_2 \le 0) \tag{18}$$

where ε_1 is the major strain of the stamped double-c element and ε_2 is the minor strain of the stamped double-c element. The wrinkling value can be calculated according to the following expression:

$$\begin{cases} q_i = \begin{cases} (-\varepsilon_2^i) - \varepsilon_1^i & (\varepsilon_1^i < (-\varepsilon_2^i)) \\ 0 & (\varepsilon_1^i > (-\varepsilon_2^i)) \end{cases} \\ y_w = \sum_{i=1}^{n} q_i^2 \end{cases} \tag{19}$$

where q_i is the wrinkling value of the ith element, ε_1^i is the major strain of the ith element, and ε_2^i is the minor strain of the ith element.

The multi-objective optimization model can be defined as:

$$\begin{aligned} Min \quad & y = w_1 f_{t-kri}(x) + w_2 f_{w-kri}(x) \\ & x \in [200, 450] \end{aligned} \tag{20}$$

where $f_{t-kri}(x)$ is the kriging value of the average thinning rate, and $f_{w-kri}(x)$ is the kriging value of the wrinkle. w_1 and w_2 are the weight coefficients of the two kriging models, and $w_1 = w_2 = 0.5$ is considered in this case.

4.2.3 Multi-objective Optimization Based on the Proposed Parallel Infilling Strategy

The VBHFs are taken as variables, and 25 initial samples are taken to construct two kriging models $f_{t-kri}(x)$ and $f_{w-kri}(x)$ based on the LHD. Some of the sampling data are given in Table 7.

New 5 samples are used to calculate the MREs of the models. The MREs of the initial kriging models are shown in Table 8. It can be seen that the MREs of the initial models are larger than 5%. Obviously, in order to obtain the optimal VBHF and improve the efficiency of the optimization, the parallel infilling strategy is used to improve the accuracy of the kriging models.

The MRE of the initial wrinkling kriging model is high, and there is a great fluctuation during the sampling process, which can be seen in Fig. 10. From Fig. 10, the kriging model construction failed and the MRE of the model increases quickly instead of gradually meeting the convergence after the 9th iteration. This phenomenon also happens to the average thinning rate kriging model. Obviously, the new sample points generated by the proposed parallel infilling strategy have a great influence on the model.

When a kriging model is being constructed, it requires that there are no repetitive points in the samples. So the redundant points must be deleted. The points with a very small Euclidean distance, called 'Pseudo Sample Points'

Table 8 Comparison of the MRE for the kriging models before and after using the parallel infilling strategy

	The MRE by initial samples (%)	The MRE by the parallel strategy (%)
Wrinkling model	86	3.95
Average thinning rate model	5.11	2.26

Table 7 Some initial sample data (force unit: KN)

	BHF1	BHF2	BHF3	BHF4	BHF5	Y	Q
1	215.12	272.93	392.56	346.23	392.38	0.0146	0.0119
2	282.55	210.46	408.02	410.80	285.52	0.0139	0.0133
3	226.06	204.22	208.37	264.54	206.68	0.0118	0.0071
4	240.94	439.16	364.79	309.91	408.58	0.0209	0.0143
5	405.27	382.42	323.48	247.39	374.41	0.0091	0.0119
…	…	…	…	…	…	…	…
21	380.46	327.93	440.44	338.70	233.65	0.0067	0.0156
22	250.30	348.59	421.85	219.82	299.04	0.0133	0.0125
23	207.08	354.88	427.92	448.43	232.61	0.0146	0.0181
24	357.78	362.91	287.61	371.11	356.63	0.0347	0.0125
25	363.99	232.64	386.68	386.26	342.49	0.0052	0.0128

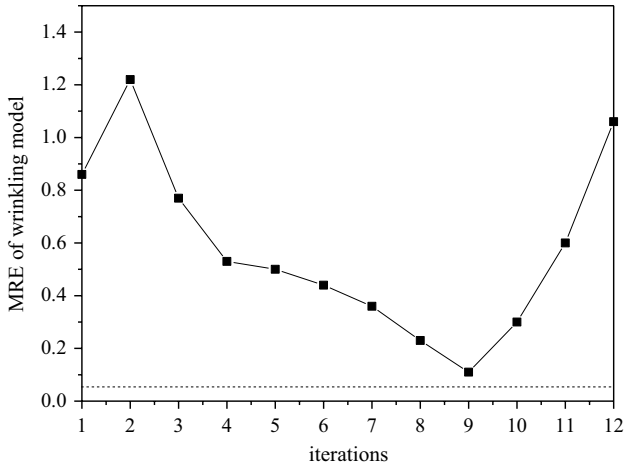

Fig. 10 The convergence process of the wrinkling kriging model before the deletion of the pseudo sample points

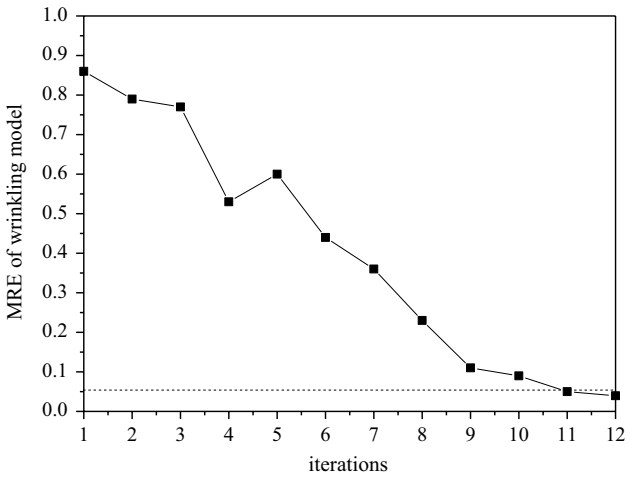

Fig. 11 The convergence process of the wrinkling model after the deletion of the PSPs

(PSP) must be deleted also, shown in Fig. 10. These PSPs are very close to the initial points, and they may have the same objective value, which directly result in the failure of constructing the models. In the double-c stamped part, the number of new points generated by the parallel strategy is 40, and 22 points are retained after deleting the PSPs. The convergence process of the wrinkling kriging model after the deletion of the PSPs is shown in Fig. 11. The MREs of the final wrinkling model and the final average thinning rate model are shown in Table 8, which shows that the MRE is reduced by 95% and 55%, respectively, compared to the

Table 9 The optimal solutions of the models before and after using the proposed parallel strategy (unit: KN)

	BHF1	BHF2	BHF3	BHF4	BHF5
The solution by the initial kriging models	360.73	417.95	376.91	450	287.13
The solution by using the proposed strategy	206.54	344.50	359.08	431.76	350.17

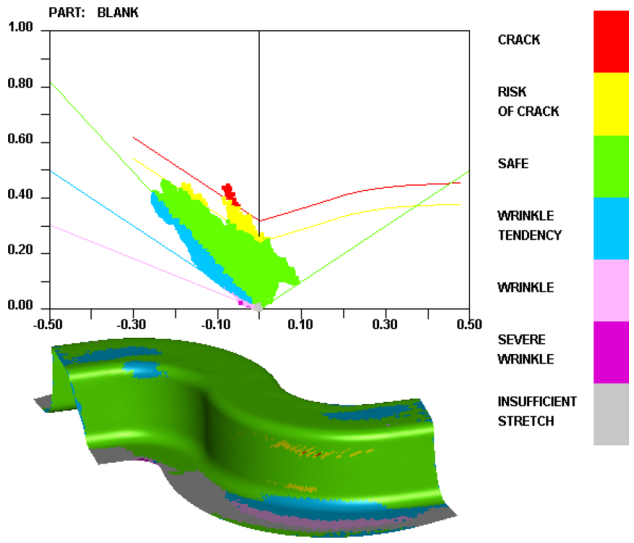

Fig. 12 The FLD of the optimal solution for the initial models

initial kriging model. It shows that the kriging model built in parallel infilling strategy has high precision.

The optimal VBHF based on the initial kriging models is obtained by WPSO, and it is shown in Table 9. The corresponding forming limit diagram (FLD) in DYNAFORM is shown in Fig. 12. It can be seen that the blank has cracked. The optimal solution of the high-precision kriging models based on the proposed parallel infilling strategy is shown in Table 9 and the FLD is shown in Fig. 13, which shows that the cracking is eliminated and the wrinkling has been reduced. The BHF can change the tangential and radial stress and strain in the flange region, thus affecting the stress and strain of the forming parts. Therefore, a reasonable VBHF can improve the sheet material formability, and eliminate or control the forming defects. The changes can be displayed in the FLDs. The result demonstrates that the optimized VBHF can better control the flow of the material, and improve its formability, eliminating or controlling the forming defects.

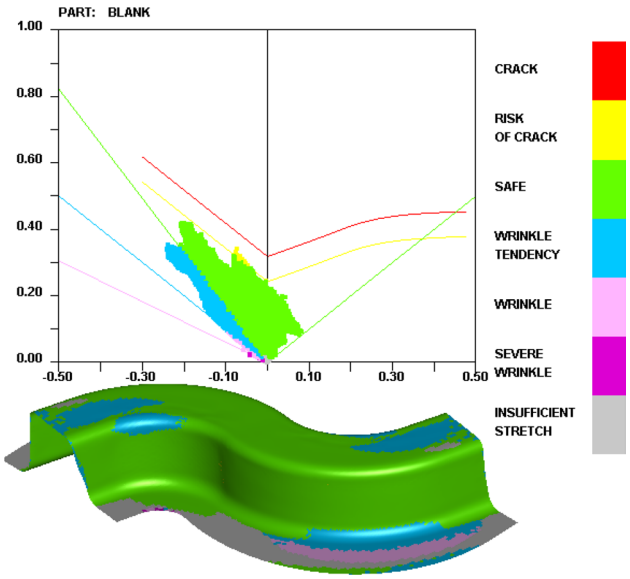

Fig. 13 The FLD of the optimal solution by the parallel strategy

5 Conclusions

In this paper, in order to improve the efficiency of constructing a kriging model with high prediction accuracy, an improved sampling criterion is proposed and a new parallel infilling strategy is presented at the same time. The following conclusions have been drawn:

(1) Based on the EI criterion, an improved infilling criterion (IEI) is proposed, and it has been demonstrated that the new criterion has better performance for finding the global maximum and higher efficiency of constructing a kriging model.
(2) Based on the EI and the IEI, a parallel infilling strategy is developed. It has been verified that the proposed parallel strategy greatly improves the efficiency of constructing kriging models with less iterations and less total sample points.
(3) The pseudo sample points (PSP) are proposed in the process of building kriging models for some practical engineering cases. PSPs and duplicate sample points should be deleted in the kriging model.
(4) The proposed parallel infilling strategy is applied to the VBHF optimization in a double-c stamped part. The optimal VBHF is quickly obtained by the WPSO based on the proposed parallel infilling strategy, and the forming quality of the double-c stamped part has been improved.

Acknowledgements The research was supported by the National Natural Science Foundation of China (NSFC51005193) and Sichuan Provincial Science and Technology Plan-Key Research and Development (Major Science and Technology Special Project) (2019YFG0313).

References

1. Liu, W., & Batill, S. (2002). *Gradient-enhanced response surface approximations using kriging models*. Atlanta: American Institute of Aeronautics and Astronautics.
2. Han, S. Q., Song, W. P., Han, Z. H., et al. (2017). Aerodynamic inverse design method based on gradient-enhanced kriging model. *Acta Aeronautica Et Astronautica Sinica, 38*(07), 138–152.
3. Kennedy, M. C., & O'Hagan, A. (2000). Predicting the output from a complex computer code when fast approximations are available. *Biometrika, 87*(1), 1–13.
4. Elsayed, K. (2015). Optimization of the cyclone separator geometry for minimum pressure drop using co-kriging. *Powder Technology, 269,* 409–424.
5. Roshan, V., Ying, H., & Sudjianto, A. (2014). Blind kriging: a new method for developing metamodels. *Journal of Mechanical Design, 130*(3), 350–353.
6. Hamza, K., Aly, M., & Hegazi, H. (2014). A kriging-interpolated level-set approach for structural topology optimization. *Journal of Mechanical Design, 136*(1), 011008.
7. Yang, L., Tong, C., Chen, C., & Guo, Q. (2017). Vibration reduction optimization of gear modification based on kriging model and genetic algorithm. *Journal of Aerospace Power, 32*(6), 1412–1418.
8. Xie, Y. M. (2014). Robust design of sheet forming process based on dynamic kriging model. *Journal of Southwest Jiaotong University, 49*(01), 160–164.
9. Kim, K. Y., & Jung, J. (2017). Multiobjective optimization for a plasmonic nanoslit array sensor using kriging models. *Applied Optics, 56*(21), 5838–5843.
10. Li, N., Cheung, S. C. P., Li, X., et al. (2017). Multi-objective optimization of HVAC system using NSPSO and kriging algorithms—A case study. *Building Simulation, 10*(5), 769–781.
11. Abebe, M., Lee, K., & Kang, B. S. (2016). Surrogate-based multipoint forming process optimization for dimpling and wrinkling reduction. *International Journal of Advanced Manufacturing Technology, 85*(1–4), 391–403.
12. Jones, D. R., Schonlau, M., & Welch, W. J. (1998). Efficient global optimization of expensive black-box functions. *Journal of Global Optimization, 13*(4), 455–492.
13. Forrester, A. I. J., & Keane, A. J. (2009). Recent advances in surrogate-based optimization. *Progress Aerospace Sciences, 45*(1–3), 50–79.
14. Laurenceau, J., Meaux, M., Montagnac, M., et al. (2010). Comparison of gradient-based and gradient-enhanced response-surface-based optimizers. *AIAA Journal, 48*(5), 981–994.
15. Liu, H., Cai, J., & Ong, Y. S. (2017). An adaptive sampling approach for kriging metamodeling by maximizing expected prediction error. *Computers & Chemical Engineering, 106,* 171–182.
16. Jia, B. Y., Yu, X. L., & Yan, Q. S. (2017). A new sampling strategy for kriging-based response surface method and its application in structural reliability. *Advances in Structural Engineering, 20*(4), 564–581.
17. Chaudhuri, A., Haftka, R. T., Ifju, P., et al. (2015). Experimental flapping wing optimization and uncertainty quantification using limited samples. *Structural & Multidisciplinary Optimization, 51*(4), 1–14.
18. Liu, J., Song, W. P., Han, Z. H., et al. (2017). Efficient aerodynamic shape optimization of transonic wings using a parallel

infilling strategy and surrogate models. *Structural & Multidisciplinary Optimization, 55*(3), 925–943.
19. Gao, Y. H., & Wang, X. C. (2012). A sequential optimization method with multi-point sampling criterion based on kriging surrogate model. *Engineering Mechanics, 29*(4), 90–95.
20. Ginsbourger, D., Riche, R.L., Carraro, L. (2007). A multi-points criterion for deterministic parallel global optimization based on kriging. In *International conference on nonconvex programming*. Rouen, France.
21. Schonlau, M. (1997). *Computer experiments and global optimization*. PhD thesis, University of Waterloo.
22. Clément, C., & Ginsbourger, D. (2013). Fast computation of the multi-points expected improvement with applications in batch selection. In *International conference on learning and intelligent optimization*. Berlin: Springer.
23. Viana, F. A. C., & Haftka, R. T. (2010). Surrogate-based optimization with parallel simulations using the probability of improvement. In *13th AIAA/ISSMO multidisciplinary analysis optimization conference*, Fort Worth, Texas, AIAA-2010-9392.
24. Yao, W., Chen, X. Q., Huang, Y. Y., et al. (2014). A surrogate-based optimization method with RBF neural network enhanced by linear interpolation and hybrid infill strategy. *Optimization Methods & Software, 29*(2), 406–429.
25. Cai, X., Qiu, H., Gao, L., et al. (2017). A multi-point sampling method based on kriging for global optimization. *Structural & Multidisciplinary Optimization, 56*(1), 71–88.
26. Desautels, T., Krause, A., & Burdick, J. W. (2014). Parallelizing exploration–exploitation tradeoffs in gaussian process bandit optimization. *The Journal of Machine Learning Research, 15*(1), 3873–3923.
27. Ma, Y., Zhou, W., & Han, Q. (2017). Research of multi-point infill criteria based on multi-objective optimization front and its application on aerodynamic shape optimization. *Advances in Mechanical Engineering, 9*(6), 1–13.
28. Wu, J., & Frazier, P. (2016). The parallel knowledge gradient method for batch Bayesian optimization. In *Advances in neural information processing systems* (pp. 3134–3142).
29. Krige, D. G. (1951). A statistical approach to some basic mine valuations problems on the Witwatersrand. *Journal of the Chemical, Metallurgical and Mining Engineering Society of South Africa, 52*(6), 119–139.
30. Henkenjohann, N., & Kunert, J. (2007). An efficient sequential optimization approach based on the multivariate expected improvement criterion. *Quality Engineering, 19*(4), 267–280.
31. Wang, D., Tan, D., & Liu, L. (2018). Particle swarm optimization algorithm: An overview. *Soft Computing, 22*(2), 387–408.
32. Mckay, M. D., Beckman, R. J., & Conover, W. J. (1979). Comparison of three methods for selecting values of input variables in the analysis of output from a computer code. *Technometrics, 21*(2), 239–245.
33. Xie, Y., Tang, W., Zhang, F., Pan, B., Yue, Y., & Feng, M. (2019). Optimization of variable blank holder force based on a sharing niching RBF neural network and an improved NSGA-II algorithm. *International Journal of Precision Engineering and Manufacturing, 20*(2), 285–299.

Yan-Min Xie received his Ph.D. degree at Shanghai Jiaotong University, China. He has been associate Professor at Southwest Jiaotong University since 2008. His research interests include robust design and process parameter optimization of sheet metal forming, numerical simulation of nonisothermal stamping for magnesium alloys, and hot forming of aluminum alloy.

Yuan-Heng Guo is a Master candidate at the School of Mechanical Engineering, Southwest Jiaotong University. His research interest is constitutive construction and numerical simulation of 2-Series Aluminum alloy under hot-working condition.

Fei Zhang received Master degree at the School of Mechanical Engineering, Southwest Jiaotong University. His research interest is CAE simulation and optimization of sheet metal forming process.

Yue-Peng Yue is a Master candidate at the School of Mechanical Engineering, Southwest Jiaotong University. His research interest is design and optimization of the blank holder in sheet metal forming.

Mei-Qiang Feng is a Master candidate at the School of Mechanical Engineering, Southwest Jiaotong University. His research interest is simulation of hot forming for 2-Series Aluminum alloy and process parameter optimization.

Jiang-Bo Zhao is a Master candidate at the School of Mechanical Engineering, Southwest Jiaotong University. His research interest is topological optimization of blank holder structure in stamping.